AGN: Taxonomy

Introduction

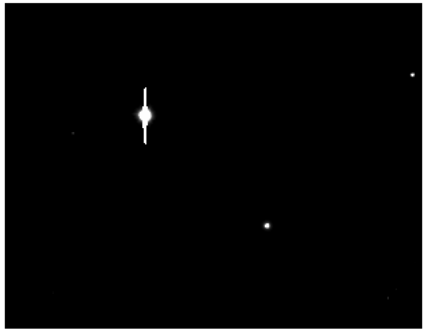

NGC 3783: *linear* intensity scale

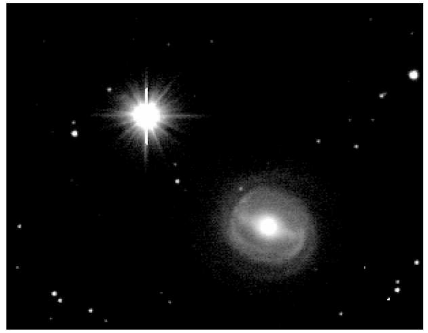

logarithmic intensity scale

Introduction

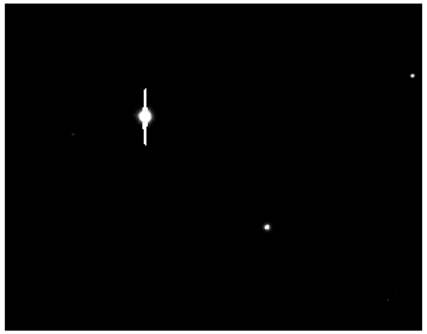

NGC 3783: *linear* intensity scale

Introduction

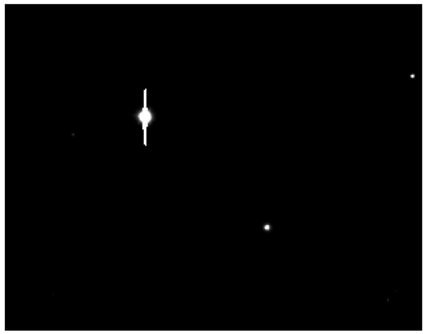

NGC 3783: *linear* intensity scale

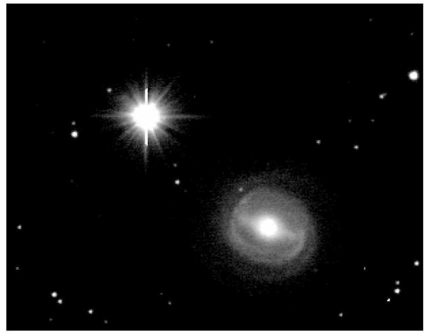

logarithmic intensity scale

Active Galactic Nuclei (AGN): Galaxies with centers as bright as a whole galaxy

NGC 1068 (M77)
(Nordic Optical Telescope)

1908: E. Fath

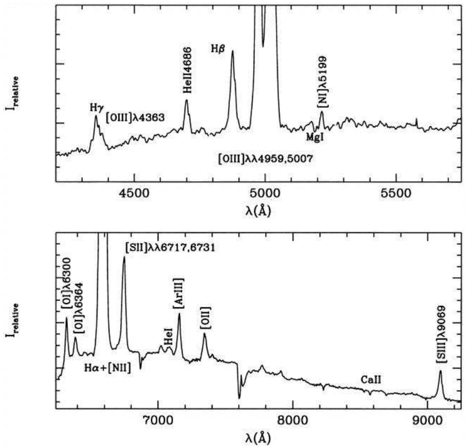

Optical spectrum of NGC 1068

(García-Lorenzo, Mediavilla & Arribas, 1999, Fig. 4)

1908: Edward A. Fath: Emission lines in NGC 1068 are similar to those seen in planetary nebulae.

Part of his dissertation!

Differences: very high degree of ionization, large line widths

1918: H. Curtis

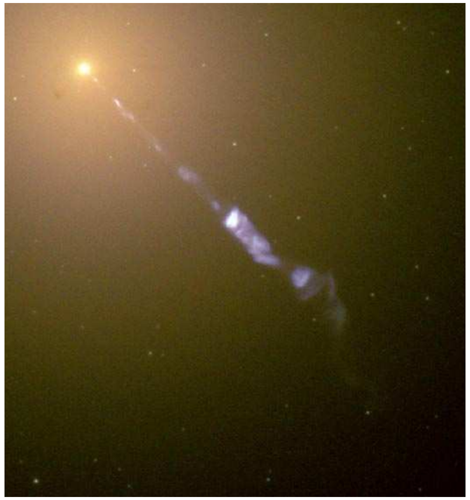

HST

1918: Heber D. Curtis: "[M87 exhibits] a curious straight ray. . . apparently connected with the nucleus by a thin line of matter".
$\Longrightarrow$ M87 contains an optical jet

1926: Edwin Hubble

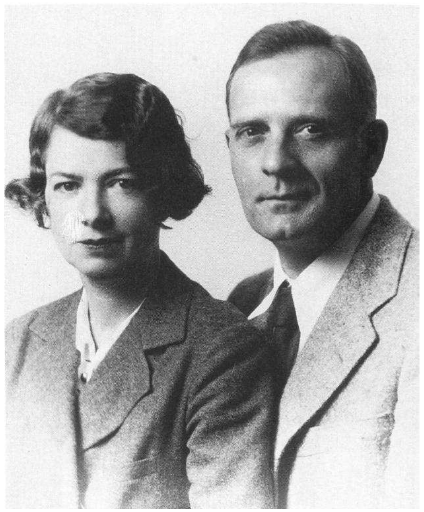

Christianson, 1995, p. 165

Edwin Hubble (1889–1953):

- Distance determination: galaxies are objects outside of our Galaxy

Hubble is the founder of modern extragalactic astronomy.

1926: Edwin Hubble

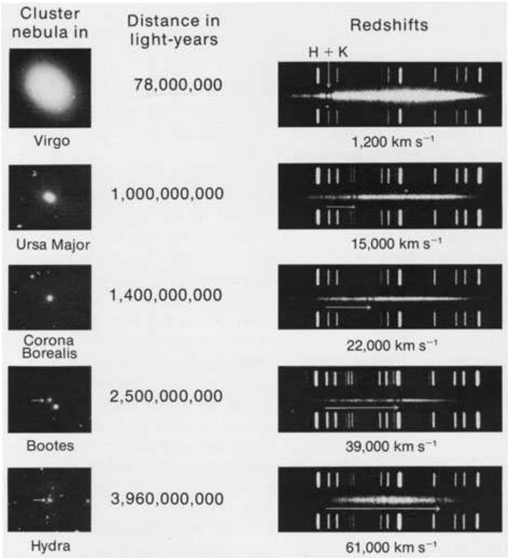

Hubble: Spectral lines are more and more redshifted with increasing distance d

Redshift:

$$z = \frac{\Delta\lambda}{\lambda} =: v/c$$

Hubble-Relation

$v = Hd$ wo $H \sim 75\,\mathrm{km\,s^{-1}\,Mpc^{-1}}$

$\Longrightarrow$ The universe expands

1943: C. Seyfert

NUCLEAR EMISSION IN SPIRAL NEBULAE*

Carl K. Seyfert†

ABSTRACT

Spectrograms of dispersion 37–200 A/mm have been obtained of six extragalactic nebulae with high-excitation nuclear emission lines superposed on a normal G-type spectrum. All the stronger emission lines from λ 3727 to λ 6731 found in planetaries like NGC 7027 appear in the spectra of the two brightest spirals observed, NGC 1068 and NGC 4151.

Apparent relative intensities of the emission lines in the six spirals were reduced to true relative intensities. Color temperatures of the continua of each spiral were determined for this purpose.

The observed relative intensities of the emission lines exhibit large variations from nebula to nebula. Profiles of the emission lines show that all the lines are broadened, presumably by Doppler motion, by amounts varying up to 8500 km/sec for the total width of the hydrogen lines in NGC 3516 and NGC 7469. The hydrogen lines in NGC 4151 have relatively narrow cores with wide wings, 7500 km/sec in total breadth. Similar wings are found for the Balmer lines in NGC 7469. The lines of the other ions show no evidence of wide wings. Some of the lines exhibit strong asymmetries, usually in the sense that the violet side of the line is stronger than the red.

In NGC 7469 the absorption K line of *Ca* II is shallow and 50 A wide, at least twice as wide as in normal spirals.

Absorption minima are found in six of the stronger emission lines in NGC 1068, in one line in NGC 4151, and one in NGC 7469. Evidence from measures of wave length and equivalent widths suggests that these absorption minima arise from the G-type spectra on which the emissions are superposed.

The maximum width of the Balmer emission lines seems to increase with the absolute magnitude of the nucleus and with the ratio of the light in the nucleus to the total light of the nebula. The emission lines in the brightest diffuse nebulae in other extragalactic objects do not appear to have wide emission lines similar to those found in the nuclei of emission spirals.

(Seyfert, 1943)

1943: Carl Seyfert: There is a class of spiral galaxies with optical *emission lines*

$\Longrightarrow$ Seyfert Galaxies

1954: W. Baade and R. Minkowski

W. Baade (Mt. Wilson Obs.)

IDENTIFICATION OF THE RADIO SOURCES IN CASSIOPEIA, CYGNUS A, AND PUPPIS A

W. Baade and R. Minkowski
Mount Wilson and Palomar Observatories
Carnegie Institution of Washington
California Institute of Technology

Received June 19, 1953

ABSTRACT

The radio sources in Cassiopeia and Puppis A are identified with a new type of galactic emission nebulosity. The outstanding features of these nebulosities are very large internal random velocities. The radio source Cygnus A is an extragalactic object, two galaxies in actual collision.

Only very few individual sources of cosmic radio emission have been identified with conspicuous astronomical objects.[1] Although the sources in Cassiopeia[2] and Cygnus A[3]

(Baade & Minkowski, 1954)

1954: Walter Baade and Rudolph Minkowski: Bright radio sources have galaxies as optical counterparts

Cyg A: 2nd brightest radio source on the sky.

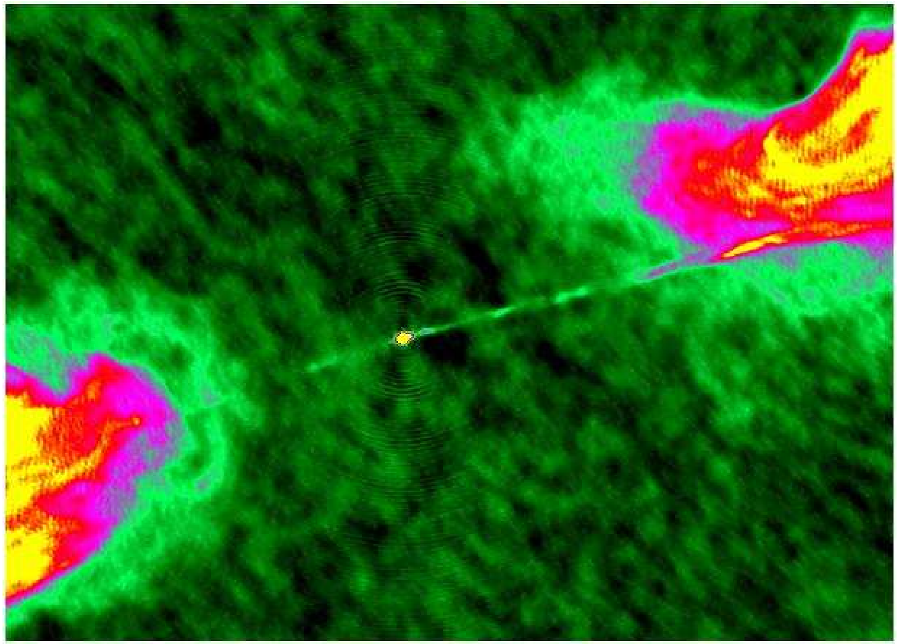

Cyg A im Radio ($\lambda = 6\,\mathrm{cm}$, VLA, Perley, Dreher & Cowan 1984)

1959: L. Woltjer

EMISSION NUCLEI IN GALAXIES

L. Woltjer*
Yerkes Observatory, University of Chicago
Received February 16, 1959

ABSTRACT

Some galaxies which show wide emission lines in the spectra of their nuclei are discussed. It is shown that, on statistical grounds, the nuclear emission must last for several times 10^8 years at least. The nuclei are extremely narrow, of the order of 100 parsecs, and, if a normal mass-to-light ratio applies, extremely massive. The width of the emission lines, which indicates velocities of a few thousand kilometers per second, is probably due to fast motions, circular or random, in the gravitational fields of the nuclei. The high star density in the nuclei may provide a source of excitation. In the nucleus of our own Galaxy the radio source Sagittarius gives evidence of strong magnetic fields and large amounts of relativistic particles. A mass of a few times 10^8 solar masses is needed to prevent disintegration of the source. The Andromeda Nebula has a nucleus with a somewhat smaller mass. The occurrence of dense nuclei may be a common characteristic of many galaxies.

(Woltjer, 1959)

1959: Lodewijk Woltjer: Objects must have very large masses.

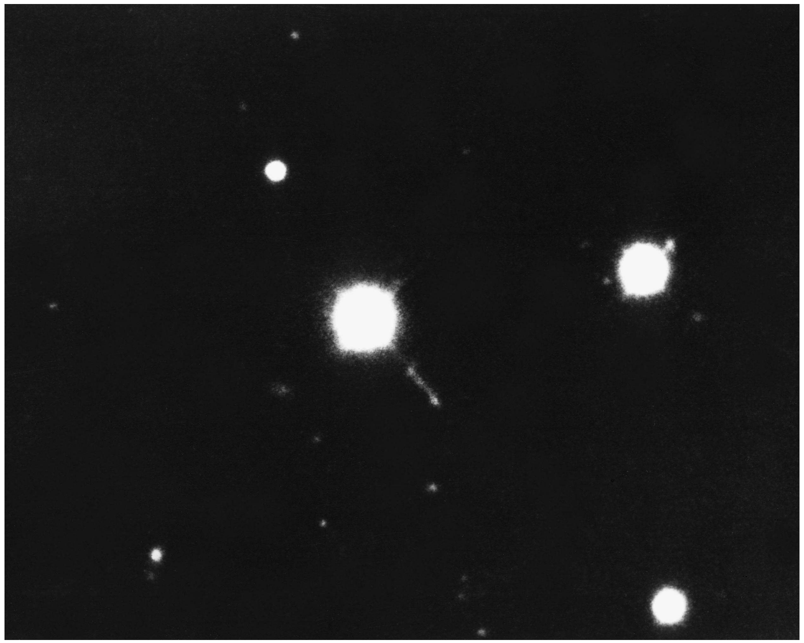

3C273 (4 m Myall telescope, NOAO/AURA/NSF)

1963: M. Schmidt

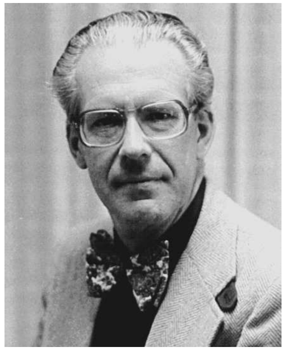

M. Schmidt (Caltech)

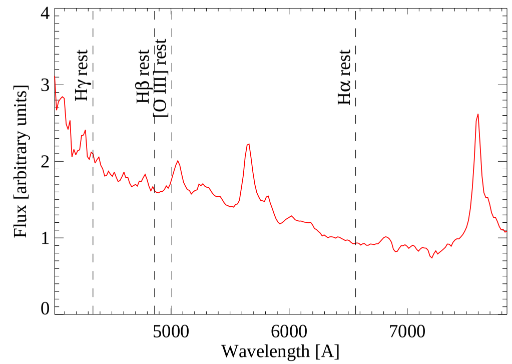

3C273 (Rondi et al., Pic du Midi)

1963: Maarten Schmidt: 3C273

1963: M. Schmidt

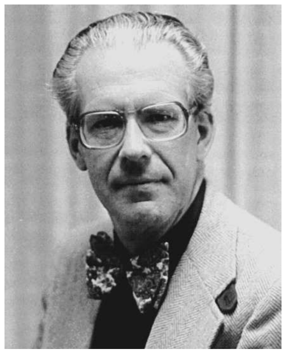

M. Schmidt (Caltech)

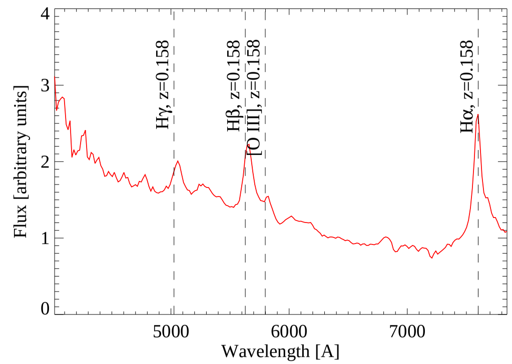

3C273 (Rondi et al., Pic du Midi)

1963: Maarten Schmidt: 3C273 has $z = 0.158 \Longrightarrow$ objects are far away!

$z = 0.158$ corresponds to $d = 1.74$ Gpc (3 billion ly)

shortly after this: 1963: J. Greenstein and Th. Matthews: 3C48 has $z = 0.368$

Seyfert Galaxies

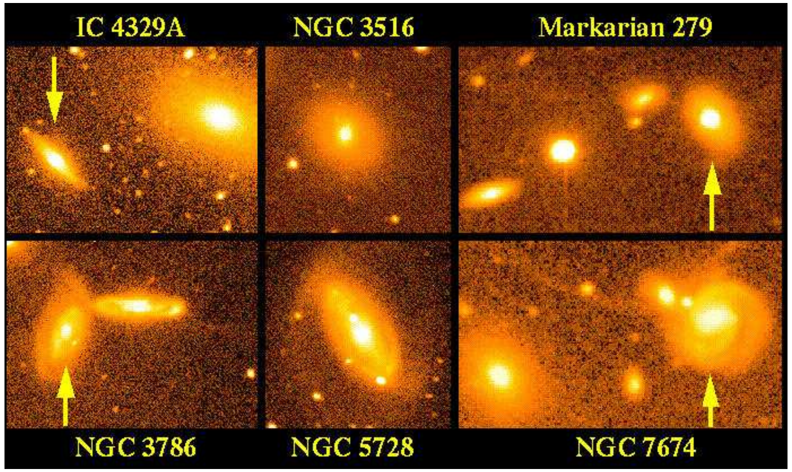

W. Keel

Seyfert Galaxien: point-like sources in the centers of galaxies, normally galaxy is detectable; two types: Seyfert 1 galaxies and Seyfert 2 galaxies.

Seyfert Galaxies

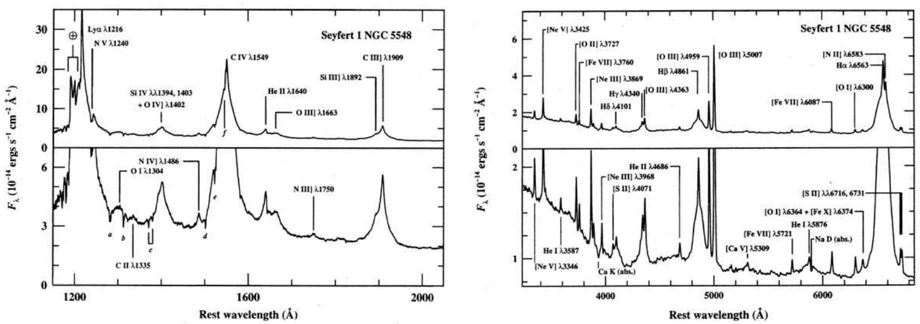

Seyfert 1 galaxies

- broad allowed lines (e.g., from H), with widths corresponding up to 10^4 km s^{-1} from a medium of high density ($n_e \gtrsim 10^9\,\mathrm{cm}^{-3}$).
- Thin forbidden lines (e.g., [O III5007]), FWHM $\sim$ few $\cdot\ 10^2$ km s^{-1} from a thin medium ($n_e \sim 10^3\,\mathrm{cm}^{-3} \dots 10^6\,\mathrm{cm}^{-3}$).

Velocity width from Doppler effect: $\Delta\lambda/\lambda = v/c$.

Seyfert 2

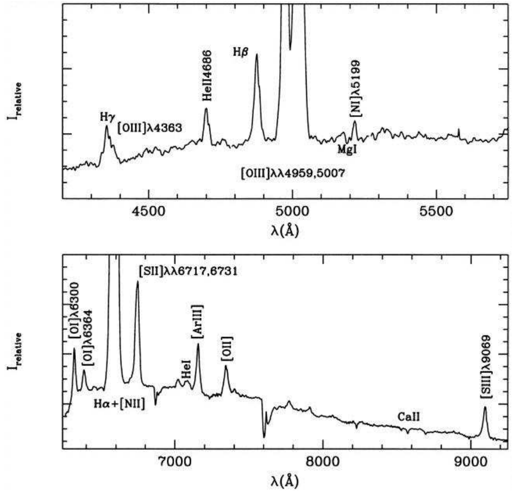

(García-Lorenzo, Mediavilla & Arribas, 1999, Fig. 4)

Spectrum of the Seyfert 2 galaxy NGC 1068:

- weak continuum (compared to Seyfert 1s).
- thin forbidden lines, $\sim$ few $\cdot\ 10^2$ km s^{-1}.
- no broad lines

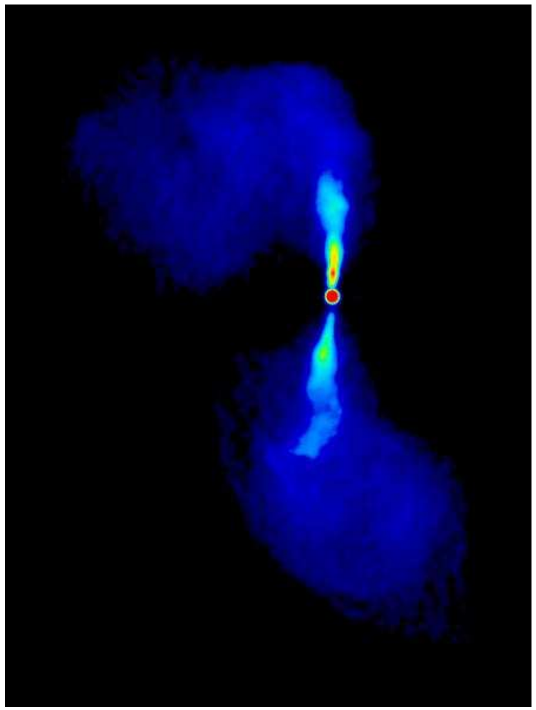

Radioimage of M84 (3C272.1): A typical Fanaroff Riley Type 1 Galaxy

Laing & Bridle (1987); VLA 4885 MHz, $134'' \times 170''$

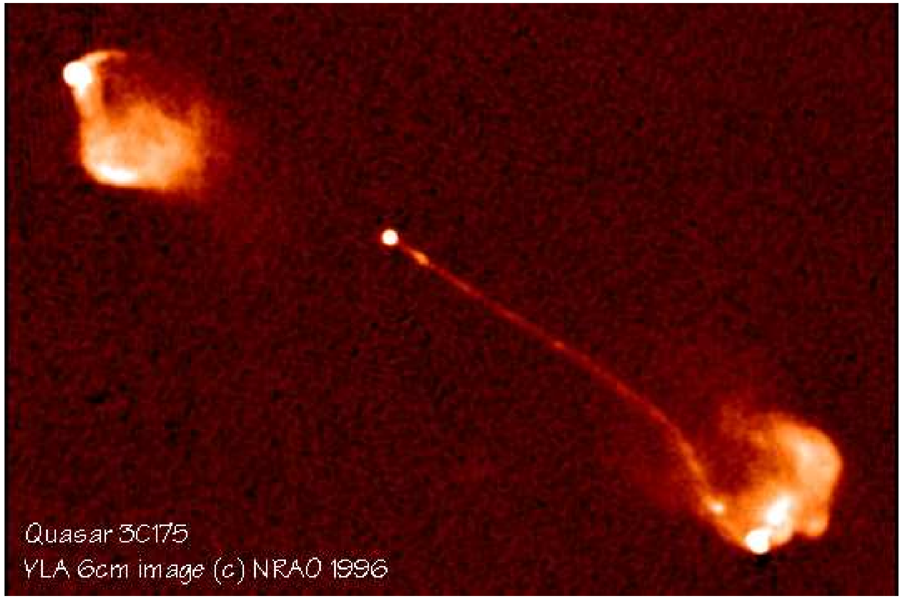

A. Bridle (priv. comm.)

Radio image of 3C175 ($z = 0.768$):
A typical FR 2 Galaxy

M87 – R. Gendler

http://www.robgendlerastropics.com/M87NM.html

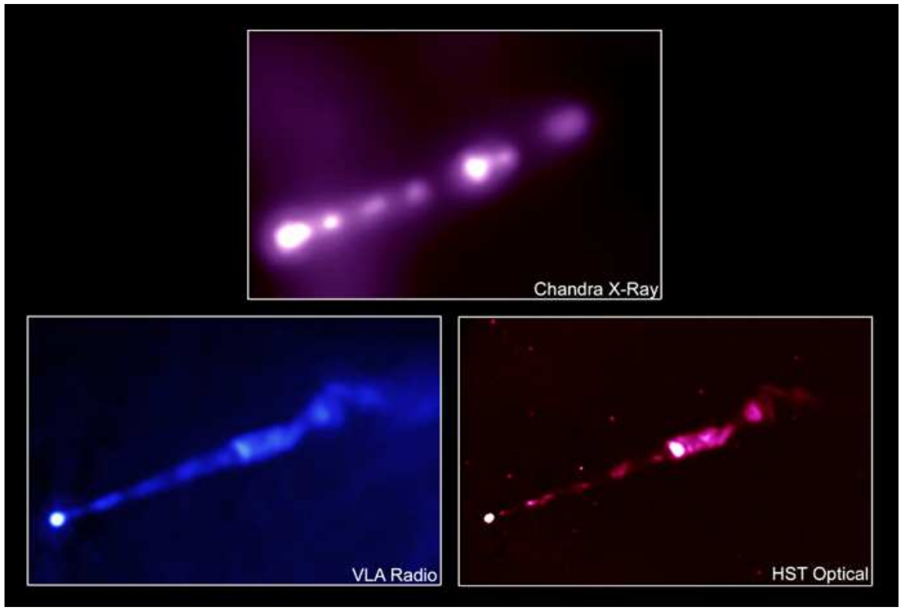

X-ray: NASA/CXC/MIT/H.Marshall et al. Radio: F.Zhou, F.Owen (NRAO), J.Biretta (STScI)
Optical: NASA/STScI/UMBC/E.Perlman et al.

Since the 1960s: multi wavelength astronomy

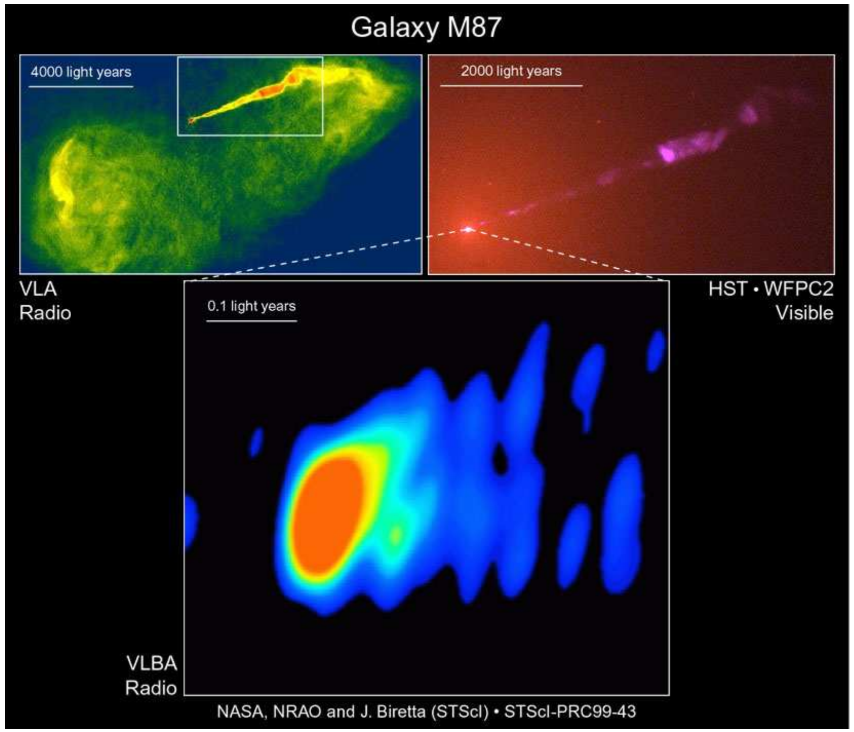

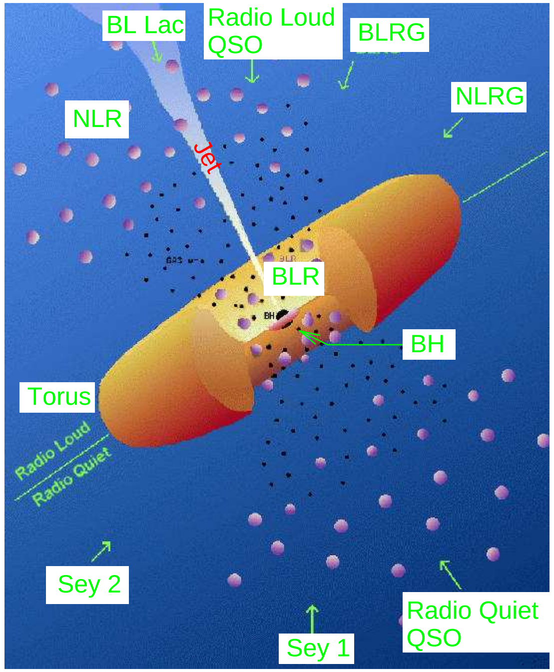

Unification: Assumes physics of all AGN is the same, phenomenology is due to different lines of sight.

(Urry & Padovani, 1995, Important: length scale is not linear!)

Baade, W., & Minkowski, R., 1954, ApJ, 119, 206
García-Lorenzo, B., Mediavilla, E., & Arribas, S., 1999, ApJ, 518, 190
Laing, R. A., & Bridle, A. H., 1987, MNRAS, 228, 557
Perley, R. A., Dreher, J. W., & Cowan, J. J., 1984, ApJ, 285, L35
Seyfert, C. K., 1943, ApJ, 97, 28
Urry, C. M., & Padovani, P., 1995, PASP, 107, 803
Woltjer, L., 1959, ApJ, 130, 38

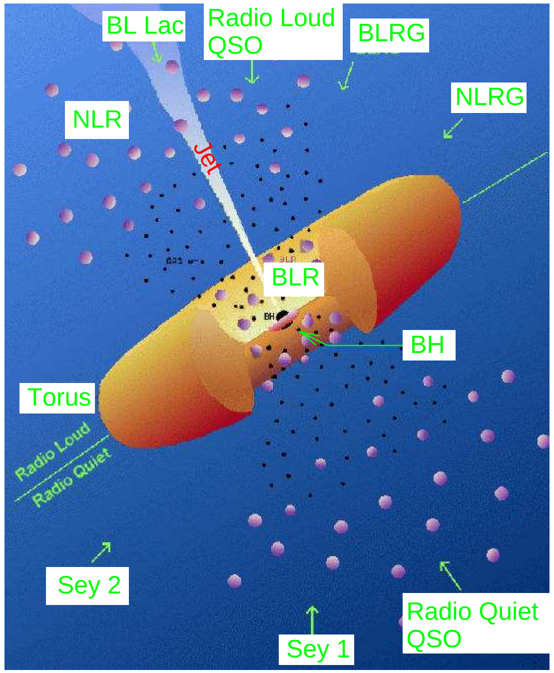

Physical properties:

Accretion disc: $r \sim 10^{-3}$ pc,
$n \sim 10^{15}\,\mathrm{cm}^{-3}$,
$kT \sim 50\,\mathrm{eV} \cdot r^{-3/4}$,
$v \sim 0.3c$ at the inner edge.

Broad Line Region (BLR): $r \sim$ 0.01–0.1 pc (=light days or less),
$n \sim 10^{10}\,\mathrm{cm}^{-3}$,
$v \sim 1000$–$5000\,\mathrm{km\,s}^{-1}$,
$T \sim 10^4\,\mathrm{K}$

Torus: $r \sim$ 1– few 10 pc,
$n \sim 10^3$–$10^6\,\mathrm{cm}^{-3}$,
T: cold

Narrow Line Region (NLR): $r \sim$ 100–1000 pc,
$n \sim 10^3$–$10^6\,\mathrm{cm}^{-3}$,
$v \sim$ few100 $\mathrm{km\,s}^{-1}$,
$T \sim 10^4\,\mathrm{K}$

Seyfert Galaxies

X-Ray Spectra

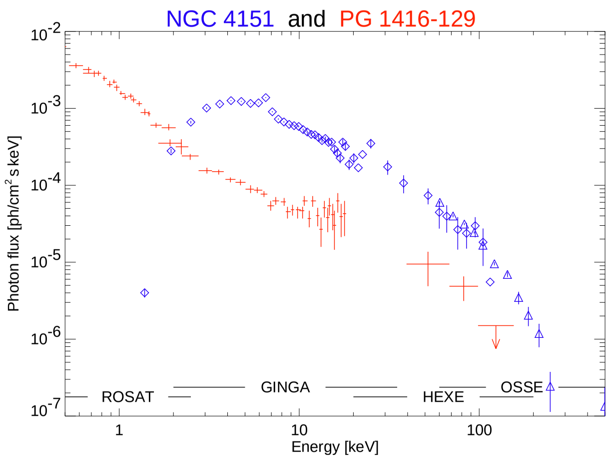

(PG 1416−129: de Kool et al., 1994, Williams et al., 1992, Staubert & Maisack, 1996; NGC 4151: Maisack 1991, 1993)

Note: NGC 4151 not corrected for interstellar absorption.

X-Ray Spectra

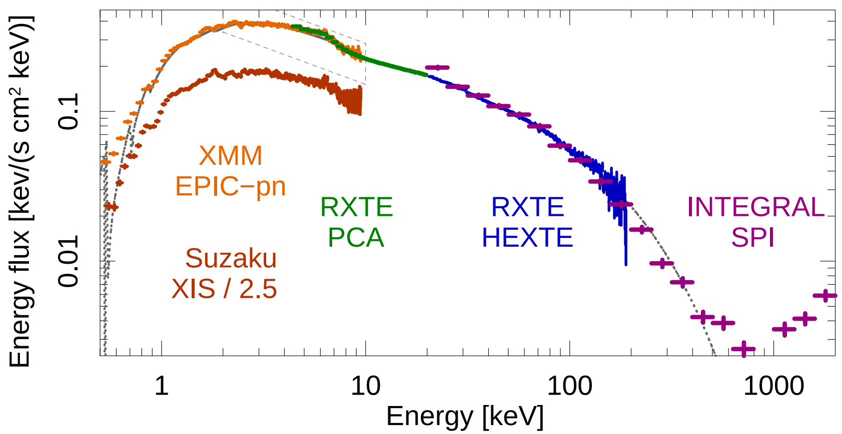

Cyg X-1 (Hanke, et al., 2008)

Spectral shape of AGN is very similar to Galactic Black Holes $\Longrightarrow$ Same physical mechanism (=Comptonization) responsible!

Reminder: Comptonization

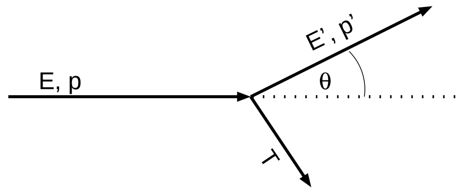

Thomson scattering: initial and final wavelength are identical.
But: in reality: light consists of photons
$\Longrightarrow$ Scattering: photon changes direction
$\Longrightarrow$ Momentum change
$\Longrightarrow$ Energy change!
This is a quantum picture
$\Longrightarrow$ Compton scattering.

Dynamics of scattering gives energy/wavelength change:

$$E' = \frac{E}{1 + \frac{E}{m_e c^2}(1 - \cos\theta)} \quad \text{or} \quad \lambda' - \lambda = \frac{h}{m_e c}(1 - \cos\theta) \tag{5.1}$$

Averaging over θ, for $E \ll m_e c^2$:

$$\frac{\Delta E}{E} \approx -\frac{E}{m_e c^2} \tag{5.2}$$

For thermal photons: energy transfer onto electron possible:

$$\frac{\Delta E}{E} = \frac{4kT - E}{m_e c^2} \tag{5.3}$$

Reminder: Comptonization

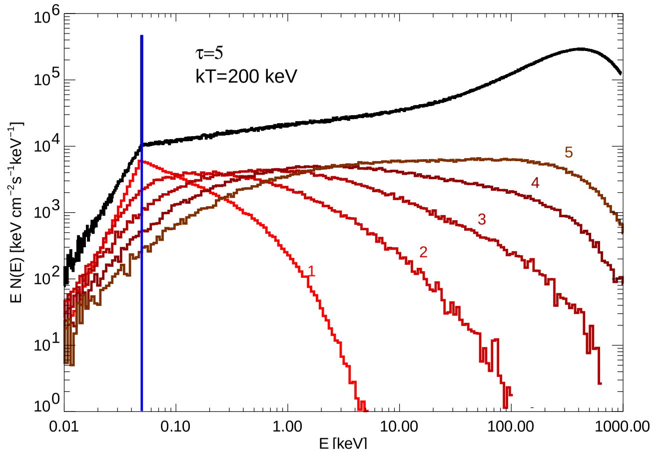

Monte Carlo simulation shows: Spectrum is $\Longrightarrow$ Power law with exponential cut-off (here: with additional “Wien hump”).

Reminder: Comptonization

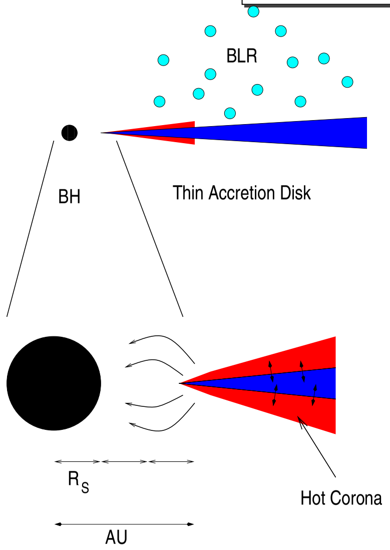

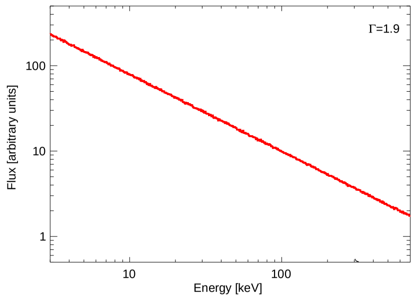

AGN X-Ray Spectrum:

- Comptonization of soft X-rays from accretion disk in hot corona ($T \sim 10^8$ K): power law continuum.

Reminder: Comptonization

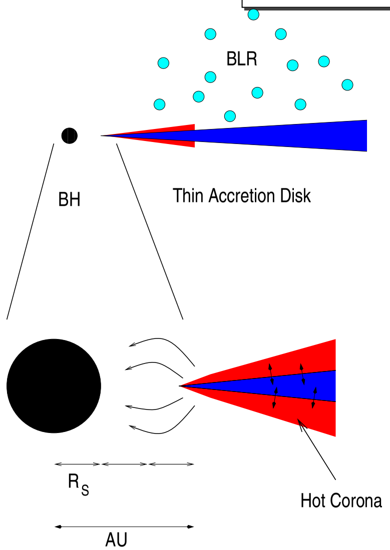

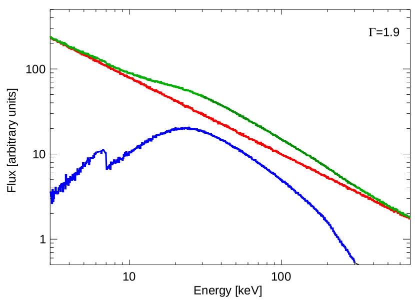

AGN X-Ray Spectrum:

- Comptonization of soft X-rays from accretion disk in hot corona ($T \sim 10^8$ K): power law continuum.
- Thomson scattering of power law photons in disk: Compton Reflection Hump

Reminder: Comptonization

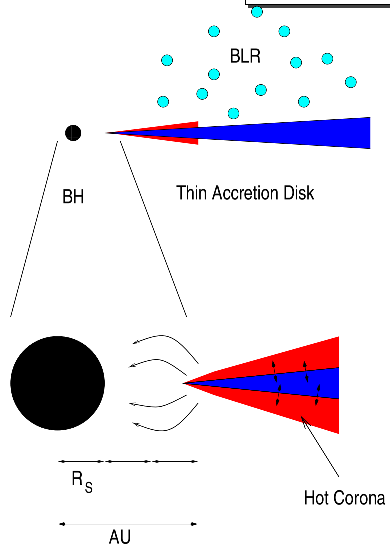

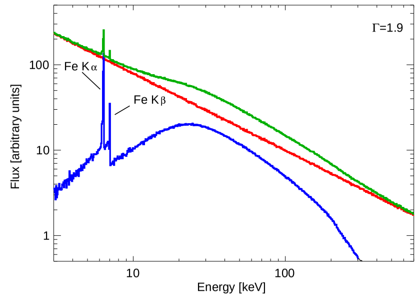

AGN X-Ray Spectrum:

- Comptonization of soft X-rays from accretion disk in hot corona ($T \sim 10^8$ K): power law continuum.
- Thomson scattering of power law photons in disk: Compton Reflection Hump
- Photoabsorption of power law photons in disk: fluorescent Fe Kα Line at ~6.4 keV

Seyfert X-Ray Spectra

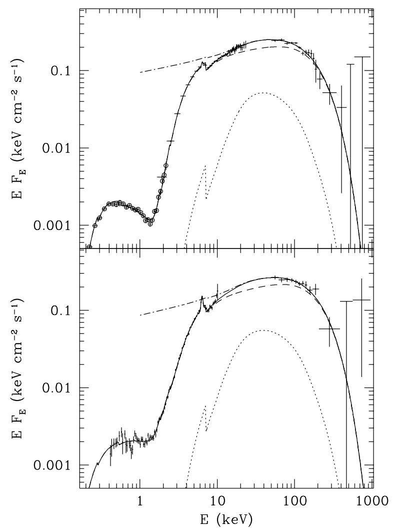

Comptonization explains broad-band Seyfert spectra very well

Example: Fits of Comptonization models to broad-band spectrum of Seyfert 1 galaxy NGC 4151 showing all three components:

- $kT_e \sim 88^{+55}_{-26}$ keV
- $N_H \sim 7 \times 10^{22}$ cm^{-2} and 13×10^{22} cm^{-2}, respectively
- Reflection factor: $\Omega/2\pi = 0.43$ (assumed; consistent with Fe line, but not significantly detected in these data [but in other AGN]).

Note strong absorption present in Seyfert 1 X-ray spectra!

(Zdziarski, Johnson & Magdziarz, 1996)

Seyfert X-Ray Spectra

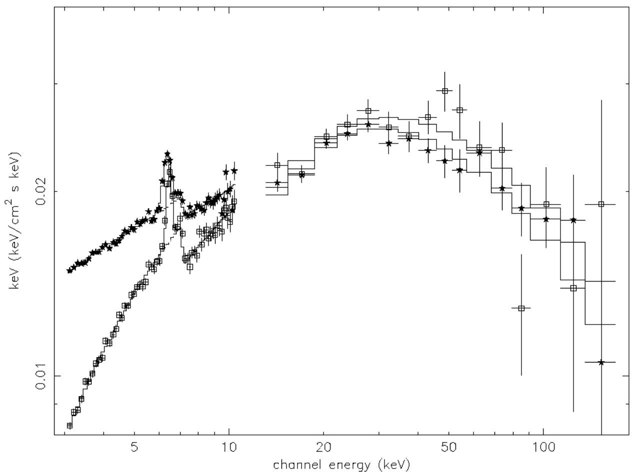

(Average Sy 1 and Sy 2 spectra from *BeppoSAX* Malizia et al., 2003, Fig. 4)

Spectra of Sy 1 and Sy 2 are very similar, except for lower N_H in Sy 2

AGN Variability

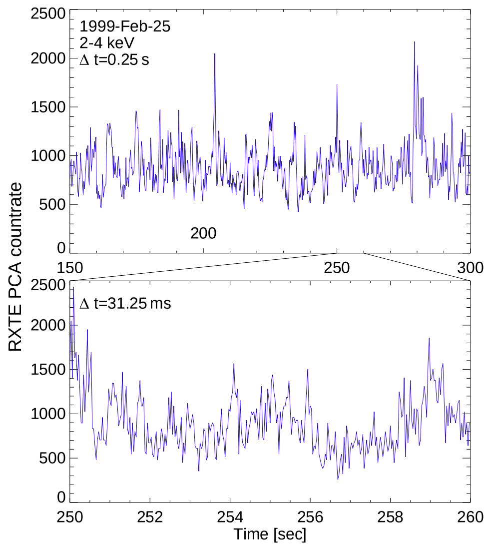

X-ray lightcurves of Galactic black holes show red-noise type variability.

Cyg X-1 with *RXTE*

AGN Variability

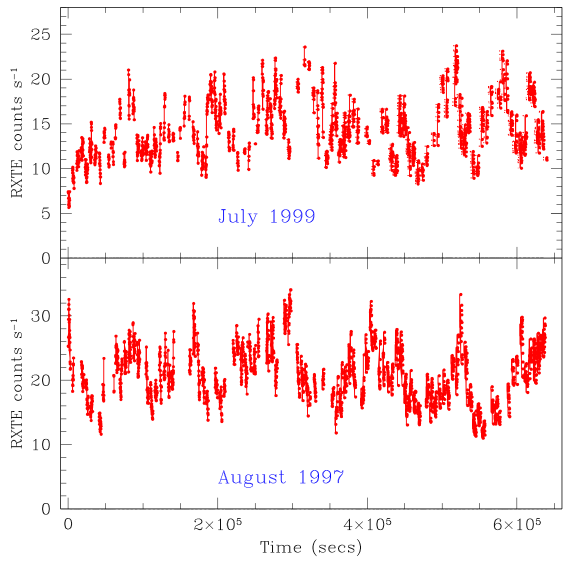

AGN lightcurves are similar to BHC lightcurves.

But on longer timescales, as expected:

Timescale at $r_\mathrm{ISCO} = 6GM/c^2$:

$$t \sim \frac{2\pi r_\mathrm{ISCO}}{\sqrt{GM/r_\mathrm{ISCO}}} \propto \frac{r^{3/2}}{M^{1/2}} \propto M \quad (5.4)$$

(MGC−6-30-15 McHardy et al., 2005)

Variability: Galactic Black Holes

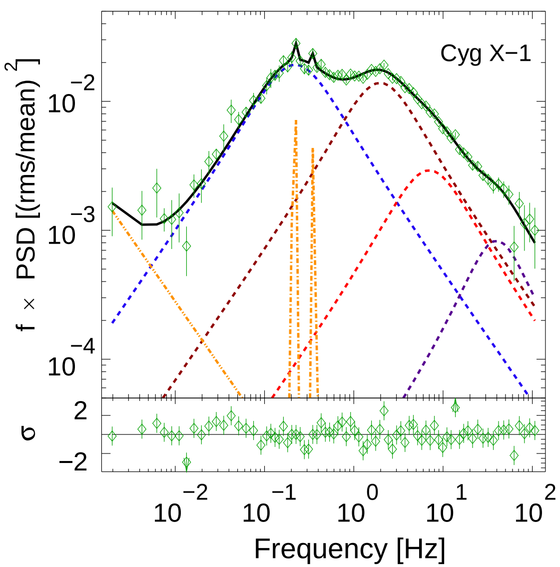

Galactic Black Holes: Power spectral density in the hard state can be well described as sum of four Lorentzians

(Nowak, 2000; Pottschmidt et al., 2003)

Variability: Galactic Black Holes

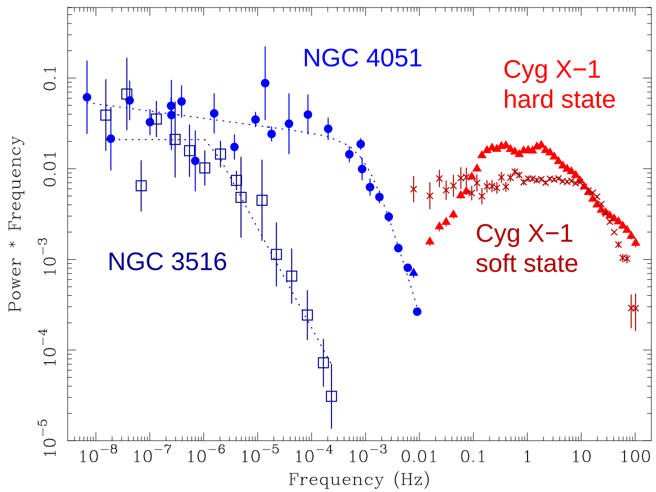

(NGC 4051; McHardy et al., 2004)

Seyfert power spectra are similar to GBH power spectra in the soft state.

PSDs can often be described by Lorentzians (Pessah, 2007)

Variability: Galactic Black Holes

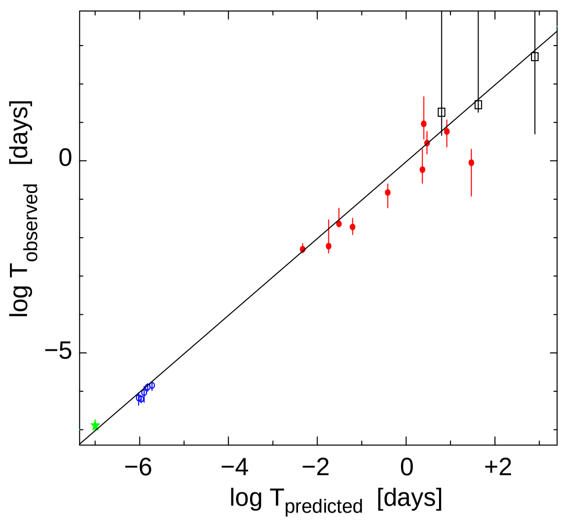

McHardy et al. (2006): Timescale of PSD break scales as

$$\log T_{\mathrm{break}} = (2.10 \pm 0.15) \log M_{\mathrm{BH}} - (0.98 \pm 0.15) \log L_{\mathrm{bol}} - (2.32 \pm 0.20)$$

Since $L_{\mathrm{bol}} \sim \dot{m}_{\mathrm{Edd}} \dot{L}_{\mathrm{Edd}}$ where $\dot{m}_{\mathrm{Edd}} = \dot{M}/\dot{M}_{\mathrm{Edd}}$:

$$T_{\mathrm{break}} \propto M_{\mathrm{BH}}^{1.12} \dot{m}_{\mathrm{Edd}}^{-0.98}$$

(McHardy et al., 2006)

Reminder: Relativistic Lines

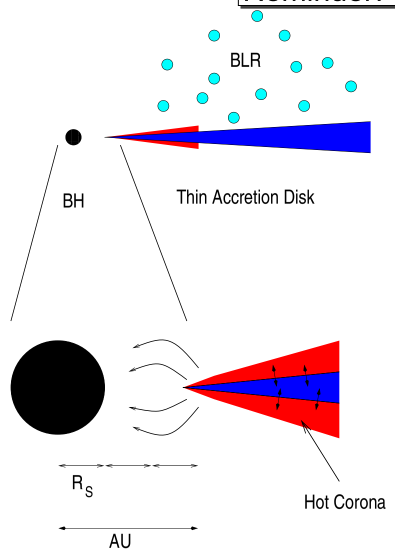

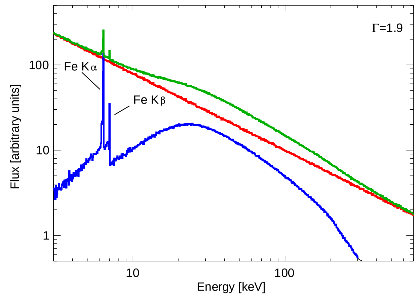

AGN X-Ray Spectrum:

- Comptonization of soft X-rays from accretion disk in hot corona ($T \sim 10^8$ K): power law continuum.
- Thomson scattering of power law photons in disk: Compton Reflection Hump
- Photoabsorption of power law photons in disk: fluorescent Fe Kα Line at ∼6.4 keV

Reminder: Relativistic Lines

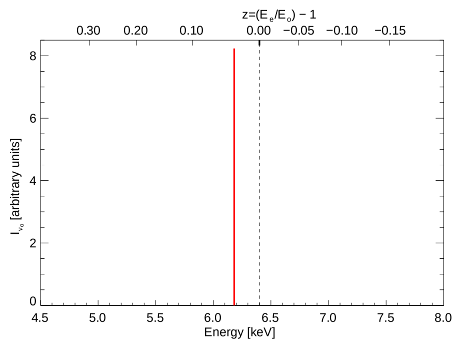

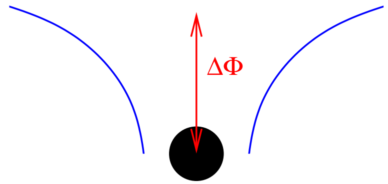

Total observed line profile affected by

- grav. Redshift

Reminder: Relativistic Lines

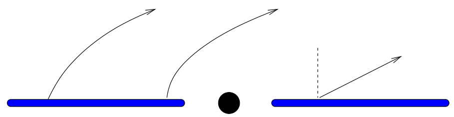

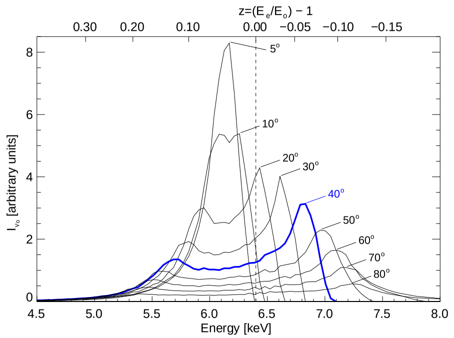

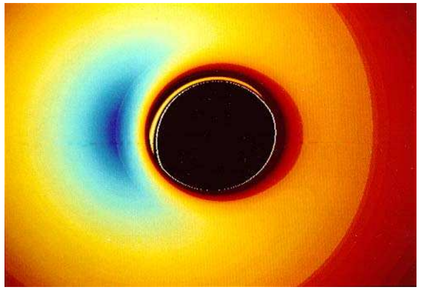

Total observed line profile affected by
- grav. Redshift
- Light bending
- rel. Doppler shift

Reminder: Relativistic Lines

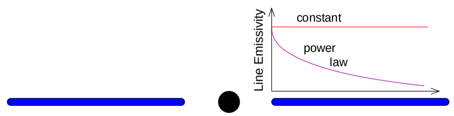

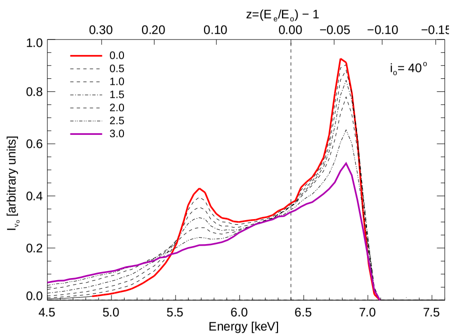

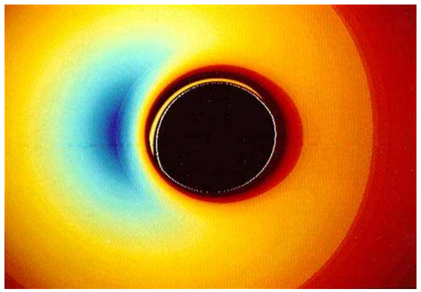

Total observed line profile affected by
- grav. Redshift
- Light bending
- rel. Doppler shift
- emissivity profile

Reminder: Relativistic Lines

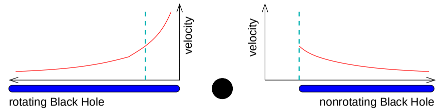

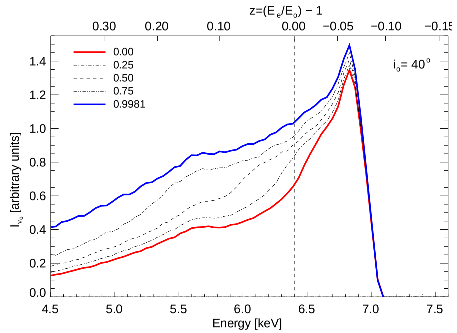

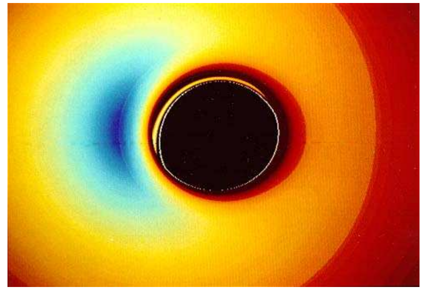

Total observed line profile affected by
- grav. Redshift
- Light bending
- rel. Doppler shift
- emissivity profile
- spin of black hole

ASCA: MCG−6-30-15

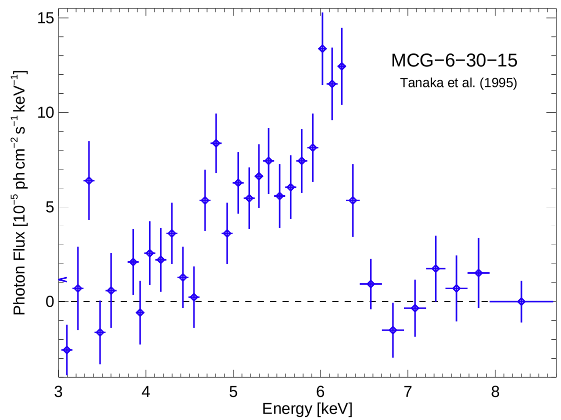

Tanaka et al. (1995): time averaged *ASCA* spectrum of Seyfert 1 MCG−6-30-15: line skew symmetric

$\Longrightarrow$ Schwarzschild black hole.

ASCA: MCG−6-30-15

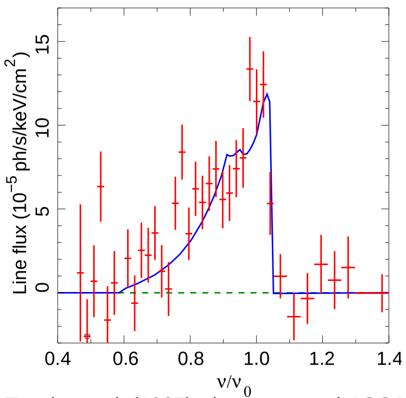

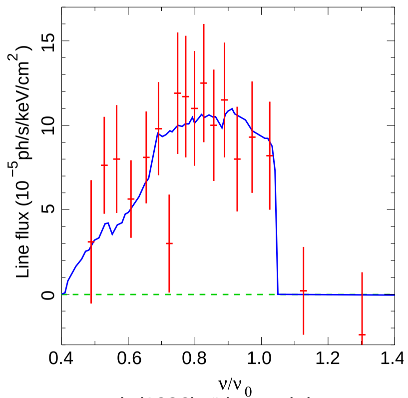

Tanaka et al. (1995): time averaged *ASCA* spectrum: line skew symmetric
$\Longrightarrow$ Schwarzschild black hole.

Iwasawa et al. (1996): "deep minimum state": extremely broad line
$\Longrightarrow$ Kerr Black Hole.

Later confirmed with *BeppoSAX* (Guainazzi et al., 1999) and *RXTE* (Lee et al., 1999).

Broad Lines with ASCA

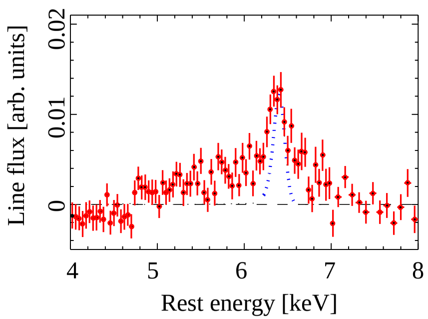

(Nandra et al., 1997, Fig. 4b)

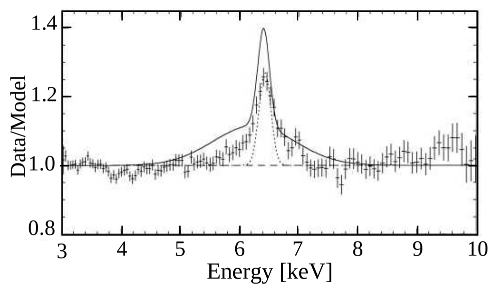

(Lubiński & Zdziarski, 2001, Fig. 2a)

ASCA: Average Seyfert Fe Kα profile contains a narrow core and a red and blue wings, but they are much weaker than MCG−6-30-15.

Best case: MCG−6-30-15

XMM: MCG−6-30-15 revisited

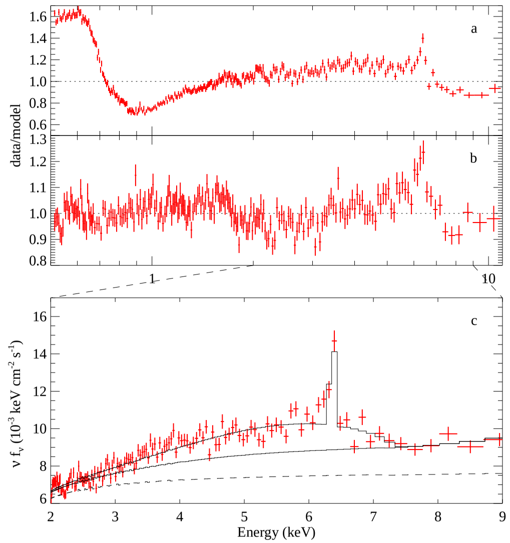

pure PL fit

Better modeling of soft excess and reflection $\Longrightarrow$ Fe Kα line has extreme width and skewed profile.

Components of the final fit.
$\Longrightarrow$ Line emissivity is strongly concentrated towards the inner edge of the disk ($\epsilon \propto r^{-4.6}$; cannot be explained with standard α-disk)

(*XMM-Newton*, June 2000, 100 ksec; Wilms et al., 2001)

XMM: MCG−6-30-15 revisited

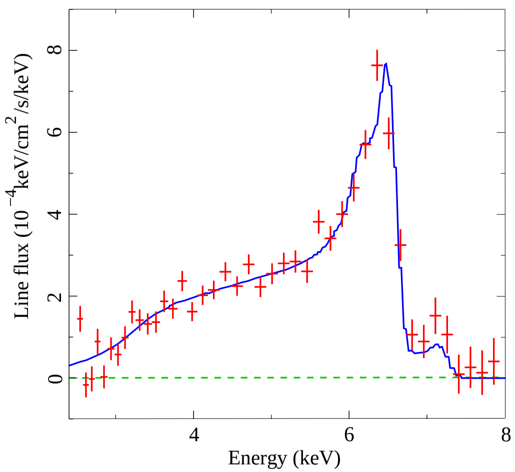

Fabian et al. (2002)

2001 July/August: 315 ksec observation (Fabian et al., 2002)

- Strong narrow line
- broad line clearly present
- emissivity profile very steep for radii close to $r_{\rm in}$

  $I_{\text{Fe K}\alpha} \propto r^{-5.5\pm0.3}$ for $r < 6.1^{+0.8}_{-0.5} r_{\rm g}$, $\propto r^{-2.7\pm0.1}$ outside that;
  Fabian & Vaughan (2003); confirms Wilms et al. (2001)

XMM: MCG−6-30-15 revisited

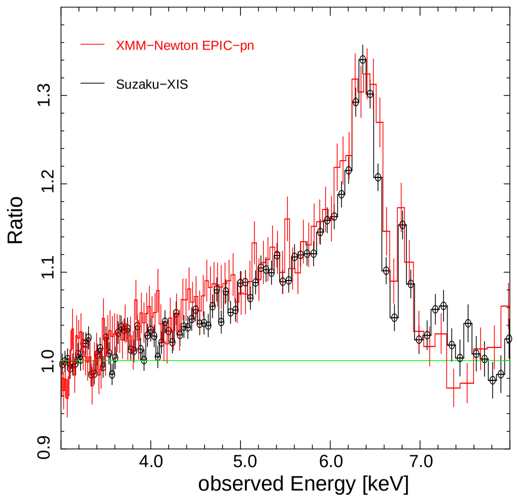

Brenneman & Reynolds (2006): Angular momentum of BH in MGC−6-30-15: $a = 0.989^{+0.009}_{-0.002}$.

Assuming no emission from inside the inner-most stable circular orbit, strongly constrained geometry.

Suzaku (2006 Jan; ~350 ksec; Miniutti et al., 2007)

Other Sources

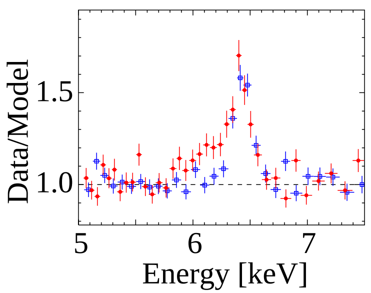

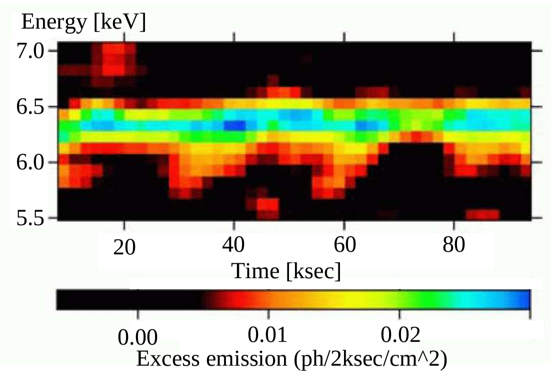

(Iwasawa, Miniutti & Fabian, 2004, Figs. 3,4)

Line profile variability in NGC 3516 $\Longrightarrow$ Corotating flare? ($7r_g \lesssim r \lesssim 16r_g$)

If interpretation is pushed further, gives $M \sim (1\ldots5) \times 10^7\,M_\odot$.

Other Sources

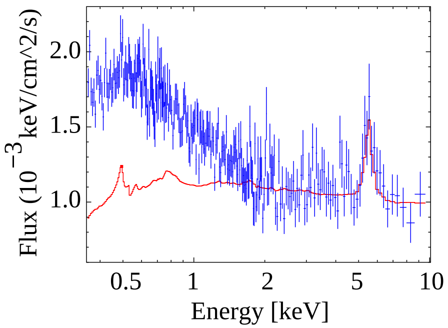

(Porquet & Reeves, 2003, Fig. 3)

XMM data from 2001

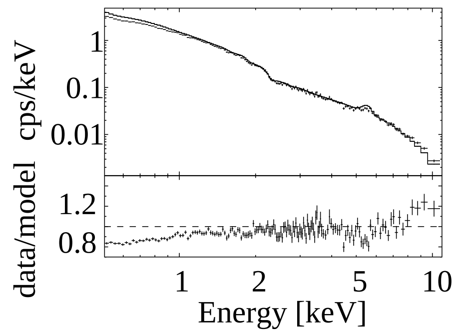

(Matt et al., 2005, Fig. 1)

comparison 2003 vs. 2001 data

Q0056−363 (broad line radio-quiet quasar, $L_X > 10^{45}\,\mathrm{erg\,s^{-1}}$):

Fe Kα has FWHM 24500 km s^{-1}, EW 275 eV

Q0056−363 is highest luminosity RQ-QSO with broad Fe Kα line.

Other Sources

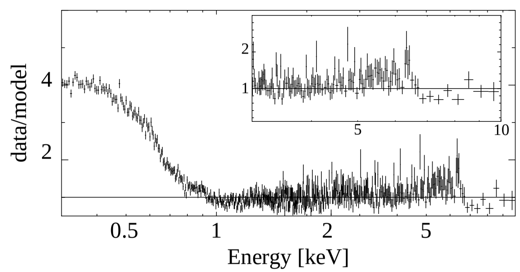

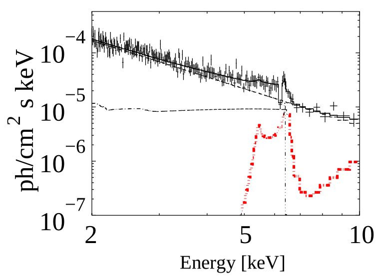

(Longinotti et al., 2003)

IRAS 13349+2436:

- Model either 2 broad emission lines *or*
- relativistic line from Fe XXIII/XXIV plus narrow absorption feature

Line shape can be rather complex!

Other examples include *blue*shifted lines, e.g., in Mkn 205 (Reeves et al., 2001) or Mkn 766.

Absorption or Lines?

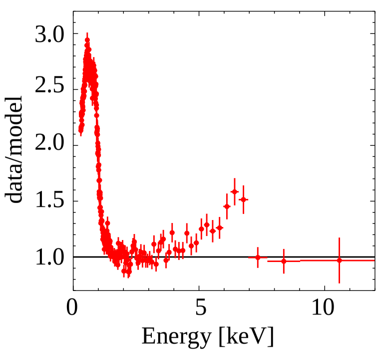

(1H0707−495; Fabian et al., 2004)

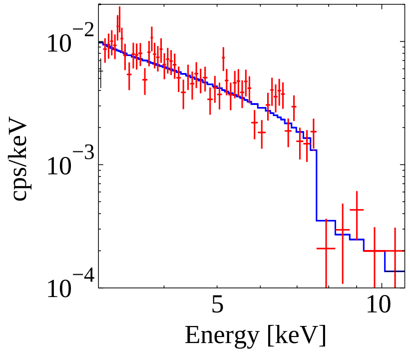

(IRAS 13224−3809; Boller et al., 2003)

Narrow Line Sy1: Strong absorption or a relativistic line fron a reflection dominated spectrum both describe the data equally well!

Similar results have been found by Pounds et al. in a variety of sources. . .

But: strong absorption models contradict observations where data >10 keV available.

Narrow Lines

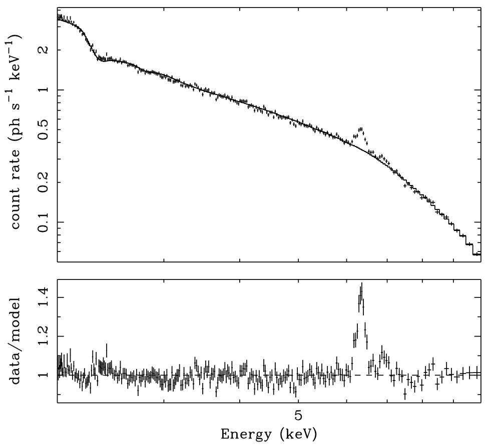

(NGC 4258; Reynolds et al. 2004)

The majority of Seyfert galaxies and QSOs do *not* show evidence for broad Fe Kα lines!

Narrow Lines

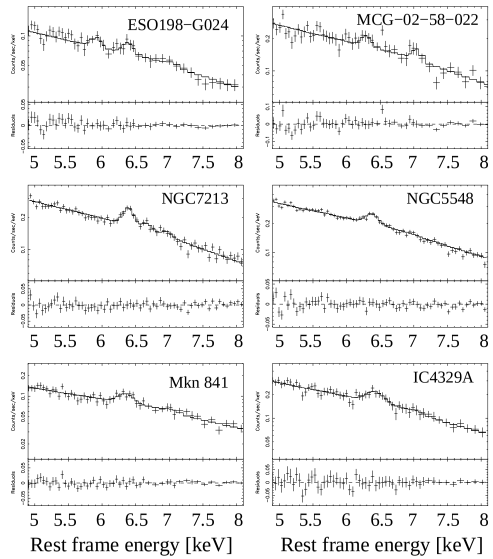

The majority of Seyfert galaxies and QSOs do *not* show evidence for broad Fe Kα lines!

Statistics for PG-QSO: 20/38 show Fe Kα line, of these 3 have broad line (Jiménez-Bailón et al., 2005)

Bianchi et al. (2004, Fig. 4)
[Sample of Seyferts with simultaneous *BeppoSAX* observations.]

5–27

Bianchi, S., Matt, G., Balestra, I., Guainazzi, M., & Perola, G. C., 2004, A&A, 422, 65

Boller, T., Tanaka, Y., Fabian, A., Brandt, W. N., Gallo, L., Anabuki, N., Haba, Y., & Vaughan, S., 2003, MNRAS, 343, L89

Fabian, A. C., Miniutti, G., Gallo, L., Boller, T., Tanaka, Y., Vaughan, S., & Ross, R. R., 2004, MNRAS, 353, 1071

Fabian, A. C., et al., 2002, MNRAS, 335, L1

Guainazzi, M., et al., 1999, A&A, 341, L27

Iwasawa, K., et al., 1996, MNRAS, 282, 1038

Iwasawa, K., Miniutti, G., & Fabian, A. C., 2004, MNRAS, 355, 1073

Jiménez-Bailón, E., Piconcelli, E., Guainazzi, M., Schartel, N., Rodríguez-Pascual, P. M., & Santos-Lleó, M., 2005, A&A, 435, 449

Lee, J. C., Fabian, A. C., Brandt, W. N., Reynolds, C. S., & Iwasawa, K., 1999, MNRAS, 310, 973

Longinotti, A. L., Cappi, M., Nandra, K., Dadina, M., & Pelletrini, S., 2003, A&A, 410, 471

Lubiński, P., & Zdziarski, A. A., 2001, MNRAS, 323, L37

Malizia, A., Bassani, L., Stephen, J. B., Di Cocco, G., Fiore, F., & Dean, A. J., 2003, ApJ, 589, L17

Matt, G., Porquet, D., Bianchi, S., Falocco, S., Maiolino, R., Reeves, J. N., & Zappacosta, L., 2005, A&A, 435, 867

McHardy, I. M., Gunn, K. F., Uttley, P., & Goad, M. R., 2005, MNRAS, 359, 1469

McHardy, I. M., Koerding, E., Knigge, C., Uttley, P., & Fender, R. P., 2006, Nature, 444, 730

McHardy, I. M., Papadakis, I. E., Uttley, P., Page, M. J., & Mason, K. O., 2004, MNRAS, 348, 783

Nandra, K., George, I. M., Mushotzky, R. F., Turner, T. J., & Yaqoob, T., 1997, ApJ, 477, 602

Nowak, M. A., 2000, MNRAS, 318, 361

Pessah, M. E., 2007, ApJ, 655, 66

Porquet, D., & Reeves, J. N., 2003, A&A, 408, 119

Pottschmidt, K., et al., 2003, A&A, 407, 1039

Reeves, J. N., Turner, M. J. L., Pounds, K. A., O'Brien, P. T., Boller, T., Ferrando, P., Kendziorra, E., & Vercellone, S., 2001, A&A, 365, L134

Tanaka, Y., et al., 1995, Nature, 375, 659

Wilms, J., Reynolds, C. S., Begelman, M. C., Reeves, J., Molendi, S., Staubert, R., & Kendziorra, E., 2001, MNRAS, 328, L27

Zdziarski, A. A., Johnson, W. N., & Magdziarz, P., 1996, MNRAS, 283, 193